

Doped orbitally ordered systems: Another case of phase separation

K. I. Kugel,^{*} A. L. Rakhmanov,^{*} and A. O. Sboychakov

Institute for Theoretical and Applied Electrodynamics, Russian Academy of Sciences, Izhorskaya Street 13, Moscow, 125412 Russia

D. I. Khomskii^{*}

II. Physikalisches Institut, Universität zu Köln, Zùlpicher Strasse 77, 50937 Köln, Germany

(Received 30 May 2008; revised manuscript received 8 August 2008; published 14 October 2008)

A possible mechanism of electronic phase separation in the systems with orbital ordering is analyzed. We suggest a simple model taking into account an interplay between the delocalization of charge carriers introduced by doping and the cooperative ordering of orbitals favoring the electron localization at lattice distortions. The proposed mechanism is quite similar to the double exchange usually invoked for interpretation of phase separation in doped magnetic oxides like manganites, but can be efficient even in the absence of any magnetic ordering. It is demonstrated that the delocalized charge carriers favor the formation of nanoscale inhomogeneities with the orbital structure different from that in the undoped material. The directional character of orbitals leads to inhomogeneities of different shapes and sizes.

DOI: [10.1103/PhysRevB.78.155113](https://doi.org/10.1103/PhysRevB.78.155113)

PACS number(s): 71.27.+a, 64.75.Nx, 71.70.Ej, 75.47.Lx

I. INTRODUCTION

The existence of superstructures is a characteristic feature of magnetic oxides, in particular, those containing ions with orbital degeneracy, i.e., Jahn-Teller (JT) ions. In the crystal lattice, the JT ions usually give rise to the orbital ordering (OO).^{1,2} The OO is typical of insulating compounds. The electron or hole doping can destroy OO since the itinerant charge carriers favor the formation of a metallic state without OO. However, at low doping level, we have a competition between the charge localization and metallicity. It is well known that such a competition can lead to the so-called electronic phase separation (PS) with nanoscale inhomogeneities.³⁻⁵ This phenomenon is often observed, e.g., in doped manganites (antiferromagnetic insulator versus ferromagnetic metal), and is usually related to some specific type of magnetic ordering. In the usual treatment of PS, the OO is not taken into account (see, however, the discussion concerning isolated orbital and magnetic polarons⁶⁻⁹). Here we study the effect of OO on PS employing minimal models, including itinerant charge carriers in the OO background, and show that at small doping the PS may appear in systems with orbital degeneracy even without taking into account the magnetic structure. We consider this effect using two versions of the models. First, in Sec. II we study a symmetrical model analogous to the Kondo-lattice model in the double exchange limit, where the orbital variables play a role of local spins. Namely, it is supposed that localized electrons create lattice distortions, leading to the formation of OO. The conduction electrons or holes introduced by doping move in the OO background. In the second version (Sec. III), we take into account the specific symmetry of e_g type for doped electrons. For both versions, we demonstrate the possible instability of a homogeneous ground state against the formation of inhomogeneities. As a result, additional charge carriers introduced by doping favor the formation of nanoscale inhomogeneities with the orbital structure different from that in the undoped material. In Sec. IV, we determine the shapes and sizes of such inhomogeneities and demonstrate that, depending on the ratio of the electron hopping integral t and the

interorbital coupling energy J , the shape can vary drastically. For the two-dimensional (2D) case, in particular, there exists a critical value of t/J , corresponding to the abrupt transition from nearly circular to needlelike inhomogeneities. This is a specific feature of orbital case: the directional character of orbitals brings about the unusual and very rich characteristics of inhomogeneous states.

II. SYMMETRICAL MODEL

Let us consider the system with JT ions having double-degenerate state. This degeneracy can be lifted by local lattice distortions, giving rise to two different states of each ion, a or b [e.g., a (b) state corresponds to elongation (compression) of anion octahedra]. The states a and b of the ion \mathbf{n} determine the corresponding orbital states of a charge carrier at this ion. In general case, each ion can be characterized by a linear combination of basis a and b states described by an angle θ ,

$$|\theta\rangle = \cos\frac{\theta}{2}|a\rangle + \sin\frac{\theta}{2}|b\rangle. \quad (1)$$

The local distortions can interact with each other leading to some regular structure. In the simplest symmetrical case, the interaction Hamiltonian can be written in a Heisenberg-type form

$$H_{\text{OO}} = J \sum_{\langle \mathbf{nm} \rangle} \tau_{\mathbf{n}} \tau_{\mathbf{m}}, \quad (2)$$

where $\tau_{\mathbf{n}} = \{\tau_{\mathbf{n}}^x, \tau_{\mathbf{n}}^z\}$ are the Pauli matrices, and a and b states of the ion \mathbf{n} correspond to eigenvectors of operators $\tau_{\mathbf{n}}^z$, with eigenvalues 1 and -1 , respectively. For Hamiltonian (2), two simplest kinds of ordering are possible: ferro-OO (the same state at each site) and antiferro (AF)-OO (alternating states at neighboring sites). In the absence of charge carriers, the ground state is antiferro-OO if $J > 0$ and ferro-OO if $J < 0$. Of course, in real materials with JT ions, the orbital Hamiltonians are more complicated, but the analysis based on

model (2) seems to be sufficient to reproduce the essential physics related to orbital ordering.

Under doping, itinerant charge carriers appear in the system, so the density of charge carries $n \neq 0$. We assume that the charge carriers are doped into double-degenerate states and move in the OO background determined by localized electrons. As we argue below, the main results will be also applicable to the case where the same electrons, e.g., e_g electrons, are responsible both for the OO and for the conduction due to doping into these e_g states. The values of electron hopping integrals should depend on the states of the neighboring lattice sites. The electron Hamiltonian can be written as

$$H_{el} = - \sum_{\langle nm \rangle, \alpha, \beta, \sigma} t^{\alpha\beta} (P_{n\alpha\sigma}^\dagger a_{n\alpha\sigma}^\dagger a_{m\beta\sigma} P_{m\beta\sigma} + \text{H.c.}), \quad (3)$$

where $a_{n\alpha\sigma}^\dagger$ and $a_{n\alpha\sigma}$ are creation and annihilation operators, respectively, for the charge carriers at site \mathbf{n} with spin projection σ at orbital α . Having in mind that we are dealing with a strongly correlated electron system, we introduced in Eq. (3) projection operators P excluding double occupation of lattice sites (we consider the case $n < 1$). Below, analyzing the electron contribution to the total energy, we shall consider square lattice in the 2D case and cubic lattice in the three-dimensional (3D) case using the tight-binding approximation. Assuming that a doped electron moves so that at each site it occupies the orbital corresponding to the respective distortion at this site, and that a site corresponding to an orbital α has nearest neighbors with orbitals β and vice versa, we can write the spectrum of charge carriers as

$$E(\mathbf{k}) = -t^{\alpha\beta} \frac{z}{D} \sum_{i=1}^D \cos k_i = z t^{\alpha\beta} \xi(\mathbf{k}), \quad (4)$$

where z is the number of nearest neighbors, D is the space dimensionality, k_i are the components of wave vector \mathbf{k} in the units of inverse lattice constant $1/d$, and $\xi(\mathbf{k})$ is normalized in such a way that $\xi_{\min} = -1$.

In our model, doped electrons at a JT distorted site a or b are in the corresponding orbital state $|a\rangle$ or $|b\rangle$. We can introduce three hopping integrals: t^{aa} , t^{bb} , and $t^{ab} = t^{ba} = t'$. For simplicity, let us assume that $t^{aa} = t^{bb} = t > t'$. Then, we have a competition of two factors: the formation either of a wider electron band or of an optimum OO type.

At the site \mathbf{n} in the state θ , the charge carrier has an orbital state $|\theta\rangle$ described by Eq. (1). The hopping integral between the sites characterized by orbital states $|\theta_1\rangle$ and $|\theta_2\rangle$ can be written as

$$t^{\theta_1\theta_2} = t \cos \frac{\theta_1 - \theta_2}{2} + t' \sin \frac{\theta_1 + \theta_2}{2}. \quad (5)$$

Note that the possibility of the interorbital hopping leads to the difference between Eq. (5) and the expression for the effective hopping integral in the conventional semiclassical double exchange model.¹⁰

First, we consider a homogeneous state, assuming that the orbital structure corresponds to the alternation of $|\theta_1\rangle$ and $|\theta_2\rangle$ orbitals ($J > 0$). In the mean-field approximation, we can represent the total energy per site as

$$E_{\text{tot}}(\theta_1, \theta_2) = z t^{\theta_1\theta_2} \varepsilon_0(n) + \frac{zJ}{2} \cos(\theta_1 - \theta_2), \quad \varepsilon_0(n) < 0, \quad (6)$$

where the dimensionless kinetic energy $\varepsilon_0(n)$ is determined by the type of the crystal lattice. A specific form of $\varepsilon_0(n)$ for different cases will be discussed below. We assume in this section that t, t' , and, therefore, $t^{\theta_1\theta_2}$ do not depend on the direction of hopping. In this isotropic case, $\varepsilon_0(n)$ does not depend on $\theta_{1,2}$ and we can easily calculate the orbital structure by minimization of total energy (6) with respect to angles θ_1 and θ_2 . At relatively large doping, when $|t\varepsilon_0(n)| > 2J$, we have ferro-OO state with $\theta_1 = \theta_2 = \pi/2$. In the opposite case, $|t\varepsilon_0(n)| < 2J$, the minimization yields $\theta_2 = \pi - \theta_1$, and

$$\theta_1 = \arcsin \left[\frac{|t\varepsilon_0(n)|}{2J} \right], \quad \frac{|t\varepsilon_0(n)|}{2J} < 1. \quad (7)$$

The total energy of such a canted orbitally ordered state is

$$E_{\text{tot}} = z t' \varepsilon_0(n) - \frac{z t^2}{4J} \varepsilon_0^2(n) - \frac{zJ}{2}. \quad (8)$$

Note that if $\varepsilon_0(n) = n f(n)$, where $f(n)$ varies slowly with n , then E_{tot} can have a negative curvature at least at small n , which is a signature of an instability of a homogeneous orbitally ordered state (negative compressibility).

Let us now determine function $\varepsilon_0(n)$ and analyze the dependence of the total energy on doping. For the tight-binding spectrum (4) of electrons in the lattice of the dimension D , the density of states $\rho_0(E)$ has the form

$$\rho_0(E) = \int \frac{d\mathbf{k}}{(2\pi)^D} \delta[E - \xi(\mathbf{k})] = \int_0^\infty \frac{ds}{\pi} \cos(Es) \left[J_0 \left(\frac{s}{D} \right) \right]^D, \quad (9)$$

where J_0 is the Bessel function. Then we have

$$\varepsilon_0(n) = \int_{-1}^{\mu(n)} dE E \rho_0(E), \quad (10)$$

with the chemical potential μ given by equation $n = \int_{-1}^{\mu} dE \rho_0(E)$.

At small doping, $n \ll 1$, it is possible to write $\varepsilon_0(n)$ in a simple explicit form. In 2D case $\varepsilon_0(n) \approx -n + \pi n^2/2$. The total energy then reads

$$E_{\text{tot}} \approx -z t' n - z \left(\frac{t^2}{4J} - \frac{\pi t'}{2} \right) n^2 - \frac{zJ}{2}. \quad (11)$$

From Eq. (11), we find that $d^2 E_{\text{tot}} / dn^2 < 0$ if

$$\frac{t}{J} > \frac{2\pi t'}{t}. \quad (12)$$

This implies an instability of the homogeneous orbitally canted state toward the phase separation into phases with ferro- and antiferro-orbital ordering. The situation here is quite similar to that for the usual double exchange (in the simplest single-band case),¹¹ which corresponds to $t' = 0$. Otherwise, when $2\pi t' / t > t/J$, a homogeneous state is stable

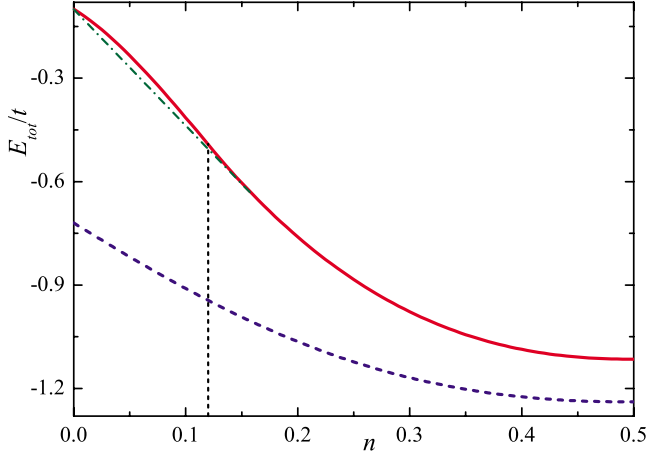


FIG. 1. (Color online) Two types of behavior of the energy of homogeneous state [Eq. (8)] in 2D as functions of doping n with a region of negative curvature (red solid line, $J/t=0.05$), and without it (blue dashed line, $J/t=0.35$); $t'=0.5t$ for both curves. For the values of parameters corresponding to the solid curve, the orbitally canted state existing on the left-hand side of vertical line is unstable toward a phase separation. The Maxwell construction in a region of phase separation is shown by green dot-dashed line. The homogeneous state corresponding to the blue dashed curve is stable in the whole range of doping.

in the whole range of doping—in contrast to the usual double exchange.

Taking $\varepsilon_0(n) \approx -n$ in Eq. (7), we get a rough estimate for a region of phase separation (assuming that it ends when θ_1 becomes equal to θ_2)

$$0 < n \lesssim \frac{2J}{t}. \quad (13)$$

So, the orbitally canted state turns out to be unstable nearly in the whole range of n where the difference $\theta_2 - \theta_1 = \pi - 2\theta_1$ with θ_1 from Eq. (7) is nonzero. The situation remains qualitatively the same, if in Eq. (8) for E_{tot} we take $\varepsilon_0(n)$, calculated using density of states (9). The behavior of $E_{\text{tot}}(n)$ in 2D case is illustrated in Fig. 1.

In three dimensions, the situation is more complicated. At small doping, we have $\varepsilon_0(n) \approx -n + an^{5/3}$, where

$$a = \frac{3}{5} \left(\frac{\pi^2}{\sqrt{6}} \right)^{2/3},$$

and the total energy becomes

$$E_{\text{tot}} \approx -zt'n - z \left(\frac{t^2}{4J} - \frac{a}{n^{1/3}} \right) n^2 - \frac{zJ}{2}. \quad (14)$$

The second derivative of E_{tot} is positive at $n \rightarrow 0$ but it changes sign at

$$n_c \approx \left(\frac{5aJt'}{9t^2} \right)^3. \quad (15)$$

Taking into account the same arguments as in 2D case, we get an estimate for the phase-separation range,

$$n_c \lesssim n \lesssim \frac{2J}{t}. \quad (16)$$

We see that the presence of nonzero nondiagonal hopping t' leads to the appearance of a lower critical concentration n_c for phase separation. The Maxwell construction would lead to phase separation in a somewhat broader doping range, starting from some $n_0 < n_c$. Here, the orbital state is described by a classical vector but, nevertheless, we have the lower critical concentration for the canted state and hence for the phase separation, which in the usual double exchange model appears only if we take into account the quantum nature of core spins.¹¹

Note that inequalities (13) and (16) are valid at relatively small values of J/t ratio.

III. ANISOTROPIC MODEL

Now we study a more realistic model of e_g orbitals in the square 2D lattice. This situation is characteristic, for example, for layered cuprates such as K_2CuF_4 or manganites (La_2MnO_4 or $\text{La}_3\text{Mn}_2\text{O}_7$). We assume that an orbital exchange Hamiltonian has a Heisenberg-type form (2). Of course, in real materials (e.g., mentioned above), the orbital exchange interaction is more complicated. We believe, however, that using orbital exchange Hamiltonian in the simple Heisenberg-type form allows us to catch all essential physics. Preliminary calculations for the case of superexchange mechanism of orbital ordering¹ show that the obtained results remain qualitatively the same.

In the case of e_g orbitals, any orbital can be written as a linear combination of two basis functions $|a\rangle = |x^2 - y^2\rangle$ and $|b\rangle = |2z^2 - x^2 - y^2\rangle$: $|\theta\rangle = \cos(\theta/2)|x^2 - y^2\rangle + \sin(\theta/2)|2z^2 - x^2 - y^2\rangle$. The hopping integrals $t^{\alpha\beta}$ in Eq. (3) now depend on the direction of hopping and can be written in the form of a matrix,

$$(t_{x,y})^{\alpha\beta} = \frac{t_0}{4} \begin{pmatrix} 3 & \mp \sqrt{3} \\ \mp \sqrt{3} & 1 \end{pmatrix}, \quad (17)$$

where minus (plus) sign corresponds to x (y) direction of hopping.

Assuming again an underlying orbital structure corresponding to the alternation of $|\theta_1\rangle$ and $|\theta_2\rangle$ orbitals, we obtain the spectrum of charge carriers in the form

$$E(\mathbf{k}) = -t_0[A_x(\theta_1, \theta_2)\cos k_x + A_y(\theta_1, \theta_2)\cos k_y], \quad (18)$$

where

$$A_{x,y}(\theta_1, \theta_2) = \left| \cos\left(\frac{\theta_1 - \theta_2}{2}\right) + \cos\left(\frac{\theta_1 + \theta_2}{2} \pm \frac{\pi}{3}\right) \right|. \quad (19)$$

The total energy then reads

$$E_{\text{tot}}(\theta_1, \theta_2) = t_0[A_x(\theta_1, \theta_2) + A_y(\theta_1, \theta_2)]\varepsilon(n; \theta_1, \theta_2) + 2J \cos(\theta_1 - \theta_2), \quad (20)$$

where $\varepsilon(n; \theta_1, \theta_2) = \int_{-1}^{\mu} dE E \rho(n; \theta_1, \theta_2)$, and the density of states can be written as

$$\rho(n; \theta_1, \theta_2) = \int_0^\infty \frac{ds}{\pi} \cos(Es) J_0\left(\frac{sA_x}{A_x + A_y}\right) J_0\left(\frac{sA_y}{A_x + A_y}\right). \quad (21)$$

Note that the density of states now depends on angles θ_1 and θ_2 via functions $A_{x,y}(\theta_1, \theta_2)$. In order to find the orbital structure, one should minimize E_{tot} [Eq. (20)] with respect to θ_1 and θ_2 . The analysis shows that, at doping n less than some critical value n_1 depending on the ratio J/t_0 , the minimum of the total energy corresponds to $\theta_1=0$ and $\theta_2=\pi$, that is, we have the homogeneous antiferro-orbital structure with alternating $|x^2-y^2\rangle$ and $|2z^2-x^2-y^2\rangle$ orbitals. We ignore here anharmonic effects and higher-order interactions, which usually stabilize locally elongated octahedra with the angles, in our notation, $\theta=\pi$ and $\pm 2\pi/3$ (see Refs. 12 and 13). The energy of such a state is

$$E_{\text{tot}} = t_0\sqrt{3}\varepsilon_0(n) - 2J. \quad (22)$$

This state is locally stable, $\partial^2 E_{\text{tot}}/\partial n^2 > 0$.

At $n=n_1$, a jumplike transition to the canted state with $\theta_2=-\theta_1$ occurs, where

$$\theta_1 = \arccos\left(\frac{t_0|\varepsilon_0(n)|}{4J}\right), \quad (23)$$

and $E_{\text{tot}}(n)$ has a kink at $n=n_1$. The energy of such canted state at $n > n_1$ is

$$E_{\text{tot}} = t_0\varepsilon_0(n) - \frac{t_0^2}{4J}\varepsilon_0^2(n) - 2J. \quad (24)$$

With the further growth of n , the angle θ_1 decreases and, at $n=n_2$, which is determined by the equation $t_0|\varepsilon_0(n_2)|/4J=1$, it vanishes, $\theta_1=0$ (ferro-OO with $|x^2-y^2\rangle$ orbitals). The total energy of the system as a function of doping is shown in Fig. 2. Note that, depending on the values of parameters, the energy (24) can have either positive or negative curvature (see the inset in Fig. 2). In the former case, the homogeneous state is locally stable in the whole range of doping, but the phase separation still exists in the range of n near $n=n_1$ due to the kink in the system energy. In the second case, PS, of course, also exists (we have an instability in some range of doping, where $\partial^2 E_{\text{tot}}/\partial n^2 < 0$). Note that these two possible situations (negative curvature of E_{tot} and the kink) can lead to inhomogeneous states with quite different properties.¹⁴

IV. INHOMOGENEITIES IN THE ORBITALLY ORDERED STRUCTURES

We demonstrated above that the additional charge carriers introduced to the orbitally ordered structures can lead to the formation of an inhomogeneous state. Now, let us discuss possible types of such inhomogeneities in more detail using a model of the e_g orbitals at the sites of 2D square lattice, considered in Sec. III. We assume that each charge carrier forms a finite region of an OO structure with alternating $|\theta_1\rangle$ and $|\theta_2\rangle$ orbitals (not necessarily ferro-OO with $\theta_1=\theta_2=0$) to optimize H_{el} . The remaining part of the crystal has antiferro-OO structure with $|x^2-y^2\rangle$ and $|2z^2-x^2-y^2\rangle$ orbit-

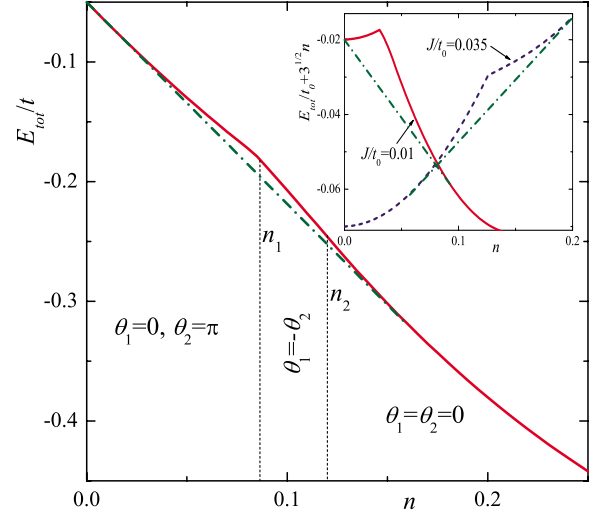


FIG. 2. (Color online) The energy of homogeneous state [Eq. (20)] for the anisotropic model as a function of doping at $J/t_0=0.025$ (red solid curve). In the region near $n_1 \approx 0.08$, the homogeneous state is unstable toward a phase separation. In the inset, the dependence of $E_{\text{tot}}(n) + t_0\sqrt{3}n$ [linear term of the dependence $E_{\text{tot}}(n)$ in the range $n < n_1$ is subtracted] on doping n is shown at the range near n_1 at different model parameters. The red solid curve (blue dashed curve) corresponds to $J/t_0=0.01$ ($J/t_0=0.035$) and has a negative (positive) value of $\partial^2 E_{\text{tot}}/\partial n^2$ in the region $n > n_1$ close to n_1 . The phase separation exists for both situations. Maxwell construction is shown by dot-dashed line.

als, according to the results in Sec. III at $n \rightarrow 0$.

The spectrum of charge carriers is given by Eq. (18). Expanding this spectrum in power series of \mathbf{k} up to the second order, we find an effective Hamiltonian for a charge carrier in a finite region,

$$\hat{H}_{\text{eff}} = -t_0(A_x + A_y) + \frac{t_0}{2} \left(A_x \frac{\partial^2}{\partial x^2} + A_y \frac{\partial^2}{\partial y^2} \right), \quad (25)$$

where A_x and A_y are given by Eq. (19). Using Hamiltonian (25), we can solve the Schrödinger equation within a finite region, which we choose in the shape of ellipse, with semi-axes $\sqrt{A_x}\rho_0$ and $\sqrt{A_y}\rho_0$. As a result, we find the following expression for the kinetic energy of a charge carrier within such droplet:

$$E_{\text{kin}} = -t_0(A_x + A_y) + \frac{t_0 j_{0,1}^2}{2\rho_0^2}, \quad (26)$$

where $j_{0,1} \approx 2.405$ is the first root of the Bessel function J_0 . The potential energy E_{pot} related to the orbital ordering is the sum of two contributions proportional to the droplet volume v ($v = \pi\sqrt{A_x A_y}\rho_0^2$), namely, the energy of the canted OO within the droplet is $(zJ/2) \cos(\theta_1 - \theta_2)$ and the loss in energy of the antiferro-OO matrix due to the formation of the droplet is $zJ/2$. As a result, we get ($z=4$),

$$E_{\text{pot}} = 4\pi\rho_0^2 J \sqrt{A_x A_y} \cos^2\left(\frac{\theta_1 - \theta_2}{2}\right). \quad (27)$$

Minimizing the droplet energy $E_{\text{kin}} + E_{\text{pot}}$ with respect to ρ_0 , we find

$$\rho_0 = \left[\frac{t_{0,1}^2}{8\pi J \sqrt{A_x A_y} \cos^2\left(\frac{\theta_1 - \theta_2}{2}\right)} \right]^{1/4}. \quad (28)$$

The total energy (per lattice site) then reads

$$E_{\text{tot}} = -2J + E(\theta_1, \theta_2)n, \quad (29)$$

$$E(\theta_1, \theta_2) = -2t_0(A_x + A_y) + j_{0,1}(8\pi t_0 J \sqrt{A_x A_y})^{1/2} \left| \cos\left(\frac{\theta_1 - \theta_2}{2}\right) \right|, \quad (30)$$

where we assume that all charge carriers introduced by doping form such identical OO droplets.

To find possible types of OO droplets, we minimize E with respect to θ_1 and θ_2 [note again, that functions $A_{x,y}$ depend on θ_1 and θ_2 according to Eq. (19)]. The function $E(\theta_1, \theta_2)$ at two different values of J/t_0 is shown in Fig. 3. In general case, the function $E(\theta_1, \theta_2)$ has several minima, and the values of θ_1 and θ_2 corresponding to the lowest minimum depend drastically on parameter J/t_0 . At small J/t_0 [Fig. 3(a)], the lowest minimum corresponds to $\theta_1 = \theta_2 = 0$, that is, we have ferro-OO structure inside the droplet with occupied $|x^2 - y^2\rangle$ orbitals. In this case, the most favorable shape of droplets is a circle [see Fig. 4(a)]. At J/t_0 larger than some critical value ($J_{\text{cr}}/t_0 \approx 0.0075$), the minimum $\theta_1 = \theta_2 = 0$ becomes metastable and the energy $E(\theta_1, \theta_2)$ has four degenerate lowest minima: two of them correspond to $\theta_1 = \pi/3$, $\theta_2 = 2\pi/3$ or $\theta_1 = -\pi/3$, $\theta_2 = -2\pi/3$, and the similar two minima with the replacement $\theta_1 \leftrightarrow \theta_2$ [see Fig. 3(b)]. In this case, we have chains of alternating $|x^2 - z^2\rangle$ and $|2x^2 - y^2 - z^2\rangle$ (or $|y^2 - z^2\rangle$ and $|2y^2 - x^2 - z^2\rangle$) orbitals and, hence, nearly one-dimensional (cigar-shaped) droplets stretched along x or y axes [Fig. 4(b)]. With the further growth of J/t_0 , the metastable state $\theta_1 = \theta_2 = 0$ splits into two states corresponding to $\theta_1^* = -\theta_2^*$ with positive and negative θ_1^* , as can be seen from Fig. 3(b). These local minima are, however, higher in energy than those corresponding to cigarlike droplets.

The existence of two types of droplets with different shapes can be easily understood. The maximum gain in the kinetic energy corresponds to the ferro-OO state with $|x^2 - y^2\rangle$ orbitals. At small J/t_0 , the kinetic energy prevails and we have circular droplets with this type of orbitals. The minimum cost in the potential energy corresponds to nearly one-dimensional structures. At larger J/t_0 , the potential energy plays more important role than the kinetic one and we get cigarlike droplets (smaller volume of such a droplet gives smaller loss of orbital energy). The orbital structure inside the droplet described above corresponds to the maximum gain in the energy for one-dimensional chain (in the absence of hopping between neighboring chains).

The analysis shows that the energy of an inhomogeneous state [Eq. (29)] consisting of circular or cigarlike OO droplets embedded into an antiferro-OO matrix is less than the

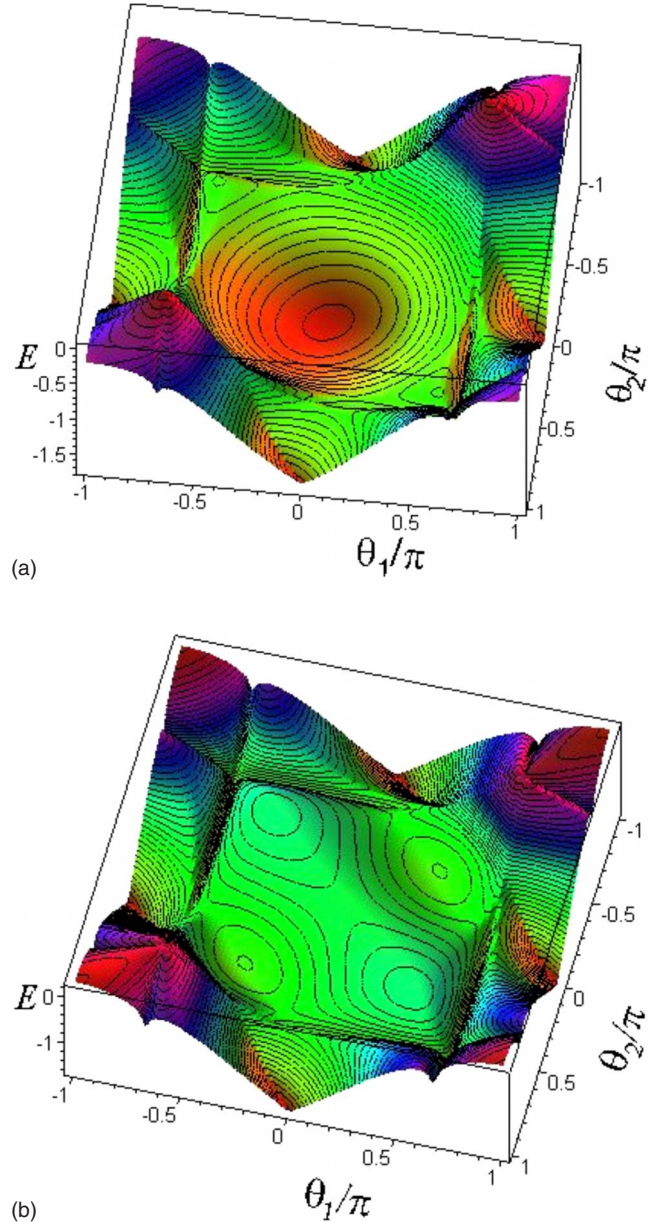


FIG. 3. (Color online) Energy [Eq. (30)] in units of t_0 as a function of angles θ_1 and θ_2 for (a) small (<0.0075) and (b) large values of J/t_0 (see the text).

energy of a homogeneous state in a certain range of doping $0 < n < n_c^*$. With the growth of the number of charge carriers, the droplets start to overlap and, at $n = n_c^*$, the inhomogeneous state of considered type (ferro-OO droplets in antiferro-OO matrix) disappears. However, the phase separation exists in a wider range of doping (see Sec. III). For circular droplets, we have an estimate $n_c^* \sim 1/\pi\rho_0^2$. Taking for estimate the ratio $J/t_0 = 0.005$, we get $\rho_0 \approx 2$ (in units of lattice constant) and $n_c^* \sim 0.08$.

In the case of cigarlike droplets, we have $A_x = 0$ (or $A_y = 0$) and according to Eq. (28) we would get that chains have infinite length (but zero volume v) $\rho_0 = \infty$. This is, of course, not a very realistic result coming from an approximation, where the potential is assumed to be proportional to the droplet volume only. In order to estimate the characteristic

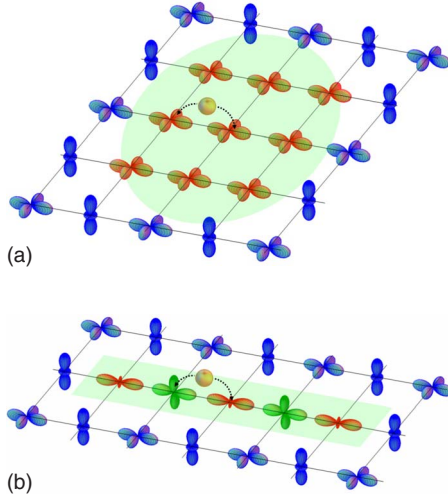


FIG. 4. (Color online) Schematic illustration of (a) circular and (b) needlelike droplets. An electron or hole moves in a finite region creating a ferro- or canted-OO structure in antiferro-OO matrix. In the case of hole, there exists a one mobile empty site within a droplet.

length L of the chain, we should take into account the surface term (proportional to the droplet's length) in the potential energy E_{pot} of the droplet. Let us consider, for definiteness, the chain of $|x^2 - z^2\rangle$ and $|2x^2 - y^2 - z^2\rangle$ orbitals stretched along x axis. In this case, we have $A_x = \sqrt{3}$ and $A_y = 0$. The effective Hamiltonian (25) is reduced to

$$\hat{H}_{\text{eff}} = -t_0\sqrt{3} + \frac{t_0\sqrt{3}}{2} \frac{\partial^2}{\partial x^2},$$

and the kinetic energy of the charge carrier in the chain of length L becomes $E_{\text{kin}} = -t_0\sqrt{3}(1 - \pi^2/2L^2)$. The surface energy of interorbital exchange interaction has a minimum, when the chain is located in an antiferro-OO matrix like what is shown in Fig. 4; each $|x^2 - z^2\rangle$ ($|2x^2 - y^2 - z^2\rangle$) orbital in the chain has its nearest-neighbor $|x^2 - y^2\rangle$ ($|2z^2 - x^2 - y^2\rangle$) orbital in the matrix. In continuum approximation, the potential energy can be written as $E_{\text{pot}} = 9JL/4$. Minimizing $E_{\text{kin}} + E_{\text{pot}}$ with respect to L , we arrive at the following formula for the characteristic length of the chain:

$$L_0 = \left(\frac{4\pi^2 t_0 \sqrt{3}}{9J} \right)^{1/3}. \quad (31)$$

At $J/t_0 = 0.05 > J_{\text{cr}}/t_0$, we have $L_0 \approx 5.5$. At random distribution of the chains in the matrix (we have chains stretched both along x and y axes), the critical concentration is about $n_c^* \sim 1/L_0^2$, but it can be larger if a more complicated structure of chains, e.g., regular stripes, appears in the system.

Similar to the situation with spin polarons, where the presence of the gapless (Goldstone) excitations leads to slowly decaying spin deformations around magnetic defect (polaron),¹⁰ we expect that the long-range strain fields will be created around orbital polarons. But, again similar to the spin case, this factor does not destroy the very self-trapped

polaron state but only would modify its parameters and also would lead to a long-range interaction between different polarons.

In this section and in Sec. III, we studied a two-dimensional case of the anisotropic model. In contrast to the isotropic model considered in Sec. II, the space dimensionality can change significantly the obtained results. Indeed, the hopping amplitudes of e_g electrons in z direction (perpendicular to the xy plane considered here) are quite different from that in xy plane. This can affect both the orbital order in the homogeneous state and the shape and the orbital structure of inhomogeneities. So, the detailed analysis of the 3D case is a special and rather complicated task.

V. CONCLUSIONS

We have studied a simple model of electronic phase separation in the system of charge carriers moving in an orbitally ordered background. It was shown that a homogeneous state in such a system can be unstable toward a phase separation, where delocalized charge carriers favor the formation of nanoscale inhomogeneities with the orbital structure different from that in the undoped material. The shapes and sizes of such inhomogeneities were determined for 2D lattice of e_g orbitals. The shape of inhomogeneities depends drastically on the ratio of interorbital exchange interaction and a hopping amplitude of the charge carriers, J/t_0 ; there exists a critical value of J/t_0 corresponding to the transition from the circular inhomogeneities to one-dimensional chains of finite length.

The model under study is quite similar to the double exchange model, where the orbital variables play a role of local spins. It is well known that such a model also exhibits an instability toward a phase separation into phases with different types of magnetic ordering. The inhomogeneous state with circular ferro-OO droplets is, in essence, an analog of a magnetic polaron state (ferromagnetic droplets in an antiferromagnetic matrix), which is usually considered in the double exchange model.^{4,5,11} Nevertheless, our orbital model is more complicated than the usual double exchange due to the existence of nondiagonal hopping amplitudes and to the anisotropy in hoppings. Both these features lead to the results specific for the orbital model, such as the kink in the energy of a homogeneous state and the canted-OO needlelike droplets. Note that the difference between spins and orbitals can have many consequences, see, e.g., Refs. 15 and 16.

Of course, in real systems with magnetic ordering, there exists the well-known conventional mechanism of formation of magnetic polarons (in simple cases—ferromagnetic microregions in an AF matrix, which decreases kinetic energy of conduction electrons). But even in this case, if there is an orbital degeneracy and if orbital ordering is present, one has to worry about orbital structure and its interplay with the motion of carriers (electrons or holes). It could be that the magnetic ordering (parallel spins) does not prevent electron motion; but if it occurs on the background of antiferro-orbital ordering (e.g., alternating $|2x^2 - y^2 - z^2\rangle$ and $|2y^2 - z^2 - x^2\rangle$ orbitals in the basal plane of manganites, which coexists with the ferromagnetic spin ordering in this plane), this AF-orbital

ordering itself will hinder electron motion—as we show—and then one has to create an orbital polaron even for the ferromagnetic spin ordering. Thus, even in the ferromagnetic state (equivalent to the spinless fermions we consider), there will still be the tendency to form orbital polarons. In principle, this is in agreement with the Monte Carlo simulations for the two-orbital model in Ref. 17, which demonstrate the possibility of phase separation in the ferromagnetic state. In the present paper, any magnetic structure and spins of the charge carriers were fully neglected. If we take into account spin degrees of freedom, it can lead to the picture with inhomogeneities with different orbital and spin configurations.

In the proposed model, the localized electrons forming an orbital order and the conduction electrons or holes were supposed to be two different groups of electrons. However, we can argue that our main results are also valid for a model, where the same electrons take part both in the hopping and in the formation of orbitally ordered structure. Indeed, in the case of magnetic oxides with Jahn-Teller ions, an orbital degeneracy is lifted by lattice distortions, giving rise to an orbitally ordered ground state at $n=1$. If we suppose that a long-range orbital ordering still exists at small hole doping $x=1-n \ll 1$, we come to the situation considered in this paper: we have holes moving in an orbitally ordered background. In a mean-field approximation, we should only replace in all formulas above $n \rightarrow x=1-n$ and $J \rightarrow J(1-x)^2$, since the number of sites taking part in interorbital exchange interaction is reduced by a factor of $1-x$. In the materials with JT ions, the orbital Hamiltonians are more complicated than the Heisenberg-type Hamiltonian considered in this paper. Preliminary calculations for the Hamiltonian corresponding to the superexchange mechanism of orbital ordering¹ show that the obtained results remain qualitatively the same.

In real substances at high doping level there may also appear an orbitally disordered state or orbital liquid, as was

proposed, e.g., for manganites, in Ref. 18; although this question is still rather controversial and other possibilities were also proposed (complex orbitals¹⁹). As we know on the better studied spin systems, disordered state is still better from the point of view of kinetic energy than the AF one (or here antiferro-orbitally ordered). But the detailed treatment of the spin case, see e.g. Refs. 3–5, has shown that in a disordered (i.e., paramagnetic) state one can gain extra energy by forming ferromagnetic polaron (“ferron”) even in the paramagnetic matrix. We expect similar situation also in our case, although this question deserves further study. To do it correctly, one has to go into all the complications and intricacies of considering electron motion in a disordered media, and this in the case of a disorder, which itself is not fixed, but can adjust to the electron. This is definitely a very interesting and rewarding but quite difficult separate problem. The lessons we have from the spin case—that polaron states are quite robust and can exist even in the disordered background—show that our general results would still be valid, so that the orbitally disordered states can compete with our polarons only for rather high doping. However, even in the absence of orbital ordering, the redistribution of charge carriers between different orbital states can lead to some unusual effects. The work in this direction is in progress.

ACKNOWLEDGMENTS

This work was supported by the European project CoMePhS (Contract No. NNP4-CT-2005-517039), International Science and Technology Center (Grant No. G1335), Russian Foundation for Basic Research (Projects No. 07-02-91567 and No. 08-02-00212), and by the Deutsche Forschungsgemeinschaft via SFB 608 and the German-Russian project (Project No. 436 RUS 113/942/0). A.O.S. also acknowledges support from the Russian Science Support Foundation.

*Also at the Department of Physics, Loughborough University, Leicestershire, LE11 3TU, UK.

¹K. I. Kugel and D. I. Khomskii, Usp. Fiz. Nauk **136**, 621 (1982) [Sov. Phys. Usp. **25**, 231 (1982)].

²M. D. Kaplan and B. G. Vekhter, *Cooperative Phenomena in Jahn-Teller Crystals* (Plenum, New York, 1995).

³E. Dagotto, *Nanoscale Phase Separation and Colossal Magnetoresistance: The Physics of Manganites and Related Compounds* (Springer-Verlag, Berlin, 2003).

⁴E. Nagaev, *Colossal Magnetoresistance and Phase Separation in Magnetic Semiconductors* (Imperial College, London, 2002).

⁵M. Yu. Kagan and K. I. Kugel, Usp. Fiz. Nauk **171**, 577 (2001) [Phys. Usp. **44**, 553 (2001)].

⁶R. Kilian and G. Khaliullin, Phys. Rev. B **60**, 13458 (1999).

⁷T. Mizokawa, D. I. Khomskii, and G. A. Sawatzky, Phys. Rev. B **63**, 024403 (2000).

⁸G. Khaliullin and S. Okamoto, Phys. Rev. Lett. **89**, 167201 (2002).

⁹J. van den Brink, G. Khaliullin, and D. Khomskii, in *Colossal*

Magnetoresistive Manganites, edited by T. Chatterji (Kluwer, Dordrecht, 2004), Chap. 6, pp. 263–302.

¹⁰P. G. de Gennes, Phys. Rev. **118**, 141 (1960).

¹¹M. Yu. Kagan, D. I. Khomskii, and M. V. Mostovoy, Eur. Phys. J. B **12**, 217 (1999).

¹²J. Kanamori, J. Appl. Phys. **31**, 14S (1960).

¹³D. Khomskii and J. van den Brink, Phys. Rev. Lett. **85**, 3329 (2000).

¹⁴C. Ortix, J. Lorenzana, and C. Di Castro, Phys. Rev. Lett. **100**, 246402 (2008).

¹⁵M. Daghofer, K. Wohlfeld, A. M. Oleś, E. Arrigoni, and P. Horsch, Phys. Rev. Lett. **100**, 066403 (2008).

¹⁶Z. Nussinov and G. Ortiz, arXiv:0801.4391 (unpublished).

¹⁷C. Şen, G. Alvarez, H. Aliaga, and E. Dagotto, Phys. Rev. B **73**, 224441 (2006).

¹⁸S. Ishihara, M. Yamanaka, and N. Nagaosa, Phys. Rev. B **56**, 686 (1997).

¹⁹J. van den Brink and D. Khomskii, Phys. Rev. B **63**, 140416(R) (2001).